

Topological lasing and self-induced transparency in two level systems

Laura Pilozzi* and Claudio Conti

Institute for Complex Systems, National Research Council (ISC-CNR), Via dei Taurini 19, 00185 Rome, Italy

The use of virtually lossless topologically isolated edge states may lead to a novel class of thresholdless lasers operating without inversion. One needs however to understand if topological states may be coupled to external radiation, and act as active cavities. We study a two-level topological insulator and show that self-induced transparency pulses can directly excite edge states. We simulate laser emission by a suitable designed topological cavity, and show that it can emit tunable radiation. For a configuration of sites following the off-diagonal Aubry-André-Harper model[1, 2], we solve the Maxwell-Bloch equations in the time domain and provide a first principle confirmation of topological lasers. Our results open the road to a new class of light emitters with topological protection for applications ranging from low-cost energetically-effective integrated lasers sources, also including silicon photonics, to strong coupling devices for studying ultrafast quantum processes with engineered vacuum.

PACS numbers: 42.65.Sf, 42.50.Md, 02.70.Bf

Introduction — In the context of transport phenomena, two or three-dimensional Bloch and Anderson models, paradigmatic for periodic and disordered structures, allow to observe a crossover from extended to localized states[3] at a critical degree of disorder [4, 5]. However, a new class of structures, the topological insulators, show a localization phase transition[6] in one-dimension (1D). Originally described in the tight-binding formulation for electrons[1], and recently for the study of localization properties of acoustic[7], electromagnetic[8–12] and matter waves[13], topological insulators are characterized by the presence of peculiar edge states, corresponding to a conducting surface for a bulk insulating material. The geometric phase of the bulk crystal determines the existence of these edge states and, correspondingly, they are protected, i.e. stable against any perturbation.

Recently the study of localization properties in topological systems has been extended to the class of resonant photonic crystals[14, 15] sustaining topologically protected boundary states [16], also involving the exciton-photon coupling[17]. The possibility of topologically protected states in resonant systems opens the challenge of realizing topologically sustained lasers, i.e. lasers based on edge states. These devices are expected to benefit of the intrinsic isolation, and hence may eventually operate at very low threshold, or without population inversion. Indeed the potential absence of loss reduces virtually to zero the gain needed for the laser operation.

In these terms, the first question to consider is if resonant topologically isolated systems can be directly excited from external inputs, and seemingly if topologically isolated states can emit coherent light into propagating modes when acting in a laser device.

In this Letter we show that a direct excitation of topological edge states is achievable in chains of two-level systems (TLS) by the use of an ultrashort self-induced transparency (SIT) pulse. Our results are based on the simulation of the Maxwell-Bloch equations [18, 19] and

we study SIT in a resonant topological insulator (RTI) where index modulation is given by either the TLS, or by the background dielectric function. In analogy with the disordered case[20], the spatial distribution of the active layers localize the SIT pulse that would otherwise induce a travelling population inversion. This localization is a fingerprint for edge states detection and sustain tunable laser emission.

Structure and edge states dispersion — A schematic of the system considered is shown in Fig. 1a). The structured region consists of resonant two-level layers A (width L_A) in an homogeneous bulk of frequency-independent dielectric function ε_b . Two configurations will be considered. In a uniform structure (US), the resonant layers, with their background dielectric function $\varepsilon_a = \varepsilon_b$, are arranged in a sequence with centers in $z_n = d_o [n + \eta d_n^H]$, where $d_n^H = \cos(2\pi\beta n + \phi)$ is the Harper modulation[2]. In a Bragg structure (BS), the resonant layers have $\varepsilon_a \neq \varepsilon_b$ and the widths b_n of the dielectric layers B are modulated as: $b_n = b_o [1 + \eta d_n^H]$.

These distributions define a 1D bichromatic periodic lattice (period d_o) modulated by a secondary lattice with

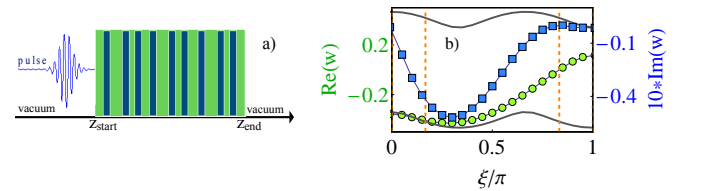


FIG. 1. (Color online) a) Sketch of the 1D chain of resonant two-level layers (blue) in an homogeneous bulk (green) of frequency-independent dielectric function ε_b . b) Real (green circles) and imaginary (blue squares) part of the left edge states frequency for $\beta = 1/3$, $\eta = 0.2/\pi$, $\omega_o = 1.533 eV$, $\varepsilon_b = 12.25$. The dashed vertical lines show the ξ values ($\xi/\pi = 0, 1/6, 5/6, 1$) where, for symmetry reasons, edge states do not exist. The continuous lines mark the gap boundaries.

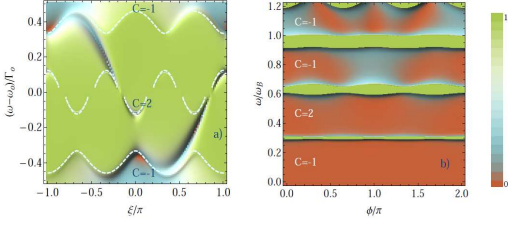


FIG. 2. Squared amplitude of the reflection coefficient $r_\infty(\phi, \omega)$ from the left side of the semi-infinite US chain a) and BS chain b) with Chern numbers C .

strength η . The phase shift ϕ governs the localization phase transition and the modulation frequency $2\pi\beta$ determines the number of topological boundary states in the gap. The structure is periodic with β^{-1} resonant layers in the unit cell and period $d = \beta^{-1}d_o$.

Uniform structure — We choose $d_o = \lambda_o/2$ with $\lambda_o = 2\pi c/(\omega_o\sqrt{\epsilon_b})$, in order to center the photonic band gap of the ordered stack ($\eta = 0$) at ω_o (TLS resonance). The A layers have radiative (non-radiative) Γ_o (Γ) decay rate, dielectric constant ϵ_a and reflection coefficient $r_A(\omega) = -i/(w + i)$, with $w = (\omega - \omega_o + i\Gamma)/\Gamma_o$, with a local Lorentz-like dispersion:

$$\chi_A(\omega) = -\frac{\hbar^2 c^2 L_A q^3}{\omega_o^2} \frac{(q^2 L_A^2 - 4\pi^2)^2}{16\pi} \frac{1}{16\pi^4 \sin^2(qL_A/2) w} \quad (1)$$

with $q = \omega\sqrt{\epsilon_a}/c$. The poles of the reflection coefficient of the whole structure give the left-edge state frequencies w_ℓ , solutions with negative imaginary part[16] of:

$$e^{2iqs_1} + (w - i)^2 e^{2iq(s_1+s_2)} + (w + i)^2 + (w^2 + 1)e^{2iqs_2} = 0. \quad (2)$$

The symmetry $w_r(\mp\xi) = w_\ell(\pm\xi)$, with $\xi = \phi - \pi/6$, gives the right-edge modes w_r . The states lay within the gap centered at ω_o with bounds given by $Tr(T) = \pm 2$, where T is the single period transfer matrix.

Figure 1b) shows the ξ dependence of the real part of the left-edge state frequency. When ξ varies in $(0, \pi)$ the edge modes traverse the band gap, bounded by the straight lines; the imaginary part $\Im[(\omega - \omega_o + i\Gamma)/\Gamma_o]$ gives their inverse lifetime.

Figure 2a) shows the reflectivity $|r_\infty(\xi, \omega)|^2$ for $\Gamma_o = 10^{-2}\omega_o$ and $\Gamma = 10^{-2}\Gamma_o$ and the corresponding Chern numbers C [21]. The edge states correspond to dips in $|r_\infty|^2$: their experimental observation requires fine spectral resolution and a high ratio between the radiative and non-radiative decay rates Γ_o/Γ . In these terms, 1D systems with weak losses and a large resonance strength Γ_o/ω_o are ideal candidates for edge-state detection.

Bragg structure — For different dielectric constants of layers A and B the spectral gaps of the structure with $\eta = 0$ at integer multiples of $\omega_B = \pi c/(L_a\sqrt{\epsilon_a} + b_0\sqrt{\epsilon_b})$ split in β^{-1} gaps. We choose $\epsilon_a = 1$ and $\epsilon_b = 12.25$, $b_0 = 200 \text{ nm}$ and $L_a = 48 \text{ nm}$, so that $\omega_B = 0.828 \text{ eV}$.

For $\beta = 1/3$ and $\eta = 0.5$, Fig. 2b) shows the reflection coefficient $|r_\infty(\phi, \omega)|^2$ from the left-edge of the semi-infinite system. Figure 3a) shows the real and imaginary part of the left-edge eigenfrequencies, and the field intensity distribution (b) for $\phi = 0.7\pi$, with the localized mode profile at $\omega = \omega_{BS}(0.7\pi)$.

Time-domain dynamics — To obtain the electric field amplitude, polarization, and population inversion we describe the dynamics of light propagation in the RTI through the Maxwell-Bloch equations:

$$\begin{aligned} \mu_0 \partial_t H_y &= -\partial_z E_x \\ \epsilon_0 \partial_t E_x &= -\partial_z H_y - \partial_t P_x \end{aligned}$$

with $P_x = 2\gamma N \rho_1$, where N is the resonant dipole density and γ is the dipole coupling coefficient, and

$$\partial_t \begin{bmatrix} \rho_1 \\ \rho_2 \\ \delta\rho_3 \end{bmatrix} = - \begin{pmatrix} \gamma_2 & -\omega_o & 0 \\ \omega_o & \gamma_2 & -2\omega_R \\ 0 & 2\omega_R & \gamma_1 \end{pmatrix} \begin{bmatrix} \rho_1 \\ \rho_2 \\ \delta\rho_3 \end{bmatrix} + \begin{bmatrix} 0 \\ 2\omega_R \rho_{30} \\ 0 \end{bmatrix} \quad (3)$$

where $\delta\rho_3 = \rho_3 - \rho_{30}$, the vector $[\rho_1 \ \rho_2 \ \rho_3]^T$ is the state density vector, with ρ_1 (ρ_2) proportional to the in-phase (in-quadrature) polarization, ρ_3 proportional to the inversion population and $\omega_R = \gamma E_x/\hbar$ the Rabi frequency; γ_1 and γ_2 denote the population and polarization relaxation rates while ρ_{30} is the initial population inversion. The corresponding susceptibility, $\chi(\omega) = -N\gamma\rho_1/(\epsilon_o E_x)$ is:

$$\chi(\omega) = \frac{2N\gamma^2}{\epsilon_o \hbar} \frac{\omega_o}{(i\omega + \gamma_2)^2 + \omega_o^2} \quad (4)$$

SIT pulse in topological insulators — Following Ref.[19] we consider the evolution of a pulse that coming from vacuum (ϵ_o) moves in the structured region of Fig. 1a) with an initial sech profile: $E_x(0, t) = E_o \text{sech}[10(t - \tau/2)/(\tau/2)] \sin[2\pi f_o t]$. We choose the pulse frequency resonant with the medium, $2\pi f_o = \omega_o/\hbar$, the pulse duration $\tau = 191 \text{ fs}$ and E_o to have a 2π pulse[24] after the reflection on the input face due to the ϵ_o, ϵ_b mismatch. The one-dimensional periodic active medium consists of N_c cells with resonant layers L_A wide, separated by slices of transparent material with

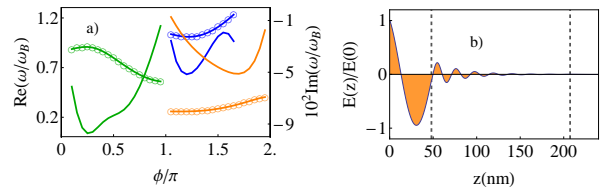


FIG. 3. (Color online) a) real (open circles) and imaginary (straight line) part of the left edge states frequency for $\beta = 1/3$, $\eta = 0.5$, $\epsilon_a = 1$, $\epsilon_b = 12.25$. b) field intensity distribution inside the system for the configuration with $\phi = 0.7\pi$.

relative permittivity $\epsilon_b = 12.25$. The dielectric layers where the TLS are not present have $\rho_{30} = 0$ and widths $s_n = z_{n+1} - z_n - L_A$ for the US and $s_n = b_n$ for the BS. We model the US system as a collection of two level atoms with density $N = 10^{24} m^{-3}$ and dipole coupling coefficient $\gamma = 1.4 \times 10^{-27} Cm$ such that $N\gamma^2 = w\Gamma_o\chi_A(\omega_o)$. Moreover we fix $\gamma_1 = \gamma_2 = 0.23$ THz. For the BS structure we choose $N = 10^{24} m^{-3}$ and $\gamma = 1 \times 10^{-29} Cm$.

We analyze the field and population inversion profile for different observation times t_i . The $E_x(z, t)$ and $\rho_3(z, t)$ plots are shown in Fig. 4 for the US chain for which $N_c = 40$ and in Fig. 5 for the BS one for which $N_c = 50$. For both the structures $z_{start} = 4\mu m$ and a $2\mu m$ layer of material ϵ_b is present at the front and rear side. To point out that the edge states are excited by the external input, we compare a topological configuration (TC) with a reference one (RC). In particular, according to the dispersion relations (Fig. 1b), 3b)), we choose:

- for the US, $\xi_{TC} = 0.5\pi$, with an edge state at the frequency $\nu_\ell = 369.4$ THz and lifetime $\tau_\ell = 0.98ps$;
- for the BS, $\phi_{TC} = 0.7\pi$ with an edge state at the frequency $\nu_\ell = 121.48$ THz and lifetime $\tau_\ell = 0.014ps$.

The reference configuration is given by the choice $\epsilon_a = \epsilon_b$ for the BS chain. In the uniform one we switch off the edge state by simply decreasing the dipole coupling coefficient. We remark that in the US the modulation in the refractive index, given by the pulse interaction with matter, is the origin of both the gap and the edge state.

In absence of an edge state, Fig. 4a), the incident laser pulse with its initial intensity and width evolve in a steady-state envelope and propagates without attenu-

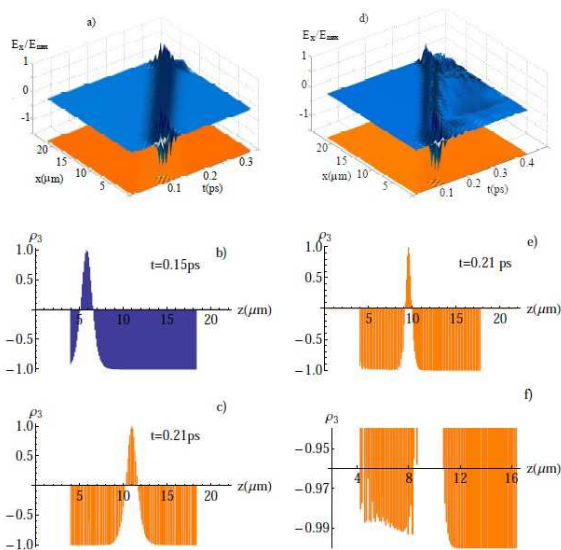


FIG. 4. Field and population inversion $\rho_3(z, t)$ spatial profile for different observation times t_i for the US structure with $\xi_{TC} = 0.5\pi$. a-c) Reference configuration with $\gamma = 1 \times 10^{-29} Cm$. d-f) Topological configuration with $\gamma = 1.4 \times 10^{-27} Cm$

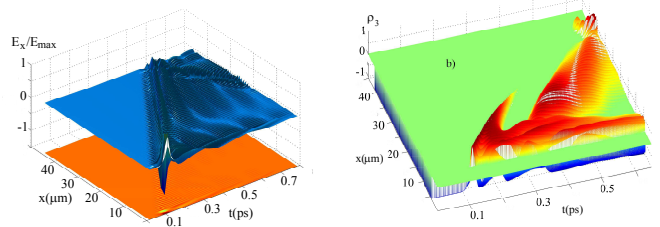


FIG. 5. Field a) and population inversion b) $\rho_3(x, t)$ spatial profile for different observation times t_i for the BS structure with $\phi_{TC} = 0.7\pi$.

ation at a constant velocity. As a consequence the maxima $\rho_3(z, t) = 1$, i.e. population inversion, Fig. 4b) and c), track, in space and time, the same path for the excitation through the structure. The BS chain gives similar results. On the contrary in the topological configuration, the localization at the input face of the spectral component of the pulse corresponding to the edge mode frequency is evident. For the US topological configuration, where the refractive index modulation is given only by the contribution of the resonance, the pulse propagates with a lower dispersion (Fig. 4d) with respect to the BS configuration (Fig. 5a). In both the cases, as a consequence of localization, the main pulse no longer meets the SIT condition and undergoes attenuation due to absorption by the TLS. The asymmetry in the $\rho_3(z, t)$ shape for the US chain, shown in Fig. 4e), and in an enlarged scale in Fig. 4f), is a fingerprint of this localization. The $\rho_3(z, t)$ shape in Fig. 5d) for the BS chain shows attenuation of the main peak and evidence for the onset of the edge mode propagation for times longer than its lifetime.

Topological lasing — Our challenge is to show that the interplay of topological localization and amplification can be exploited to design mirrorless laser systems in analogy with random structures[22]. To this end, with the resonant layers as the light-amplifying material, we study edge modes in the stimulated emission process. We start with the two-level system population initially inverted in the upper state $\rho_{30} = 1$ and add, following Ref.[23], as the only source a stochastic term with Gaussian statistic in the electric field evolution $E_x = \sqrt{-2\xi_E \ln(a)} \cos(2\pi b)$ with a and b random numbers uniformly distributed in (0,1) interval and variance $\xi_E = 10^{-3} V^2 m^{-2}$. For the BS chain, with a gap in the range $(120 \div 134)$ THz, and $\phi = 0.7\pi$, the TLS resonance frequency is $\nu_o = \nu_\ell(0.7\pi)$. Other parameters are: $N = 10^{23} m^{-3}$, $\gamma = 4.8 \times 10^{-28} Cm$, $T_1 = 1/\gamma_1 = 10^{-11} s$ and $T_2 = 1/\gamma_2 = 7 \times 10^{-15} s$. For this system, Fig. 6 a) and b) show the time-dependent output intensity in the left side of the structure, and the time-resolved spectrum. After a wide-band transient ($t \approx 1ps$), for $t \in (1 \div 30) ps$ emission is multimodal with a spectrum corresponding to delocalized Bloch modes at the PBG band-edges. At longer times ($t \gg 30 ps$), the high qual-

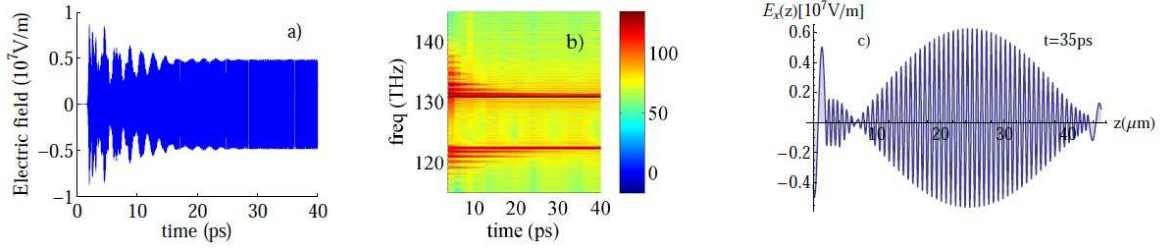


FIG. 6. a) Time-dependent output intensity in the left side of the BS chain; mode beating is observed in the time range ($1 \div 30 \text{ps}$) b) time evolution of its spectrum; c) snapshot of the electric field for $t=35 \text{ps}$.

ity factor modes survive and the spectrum is characterized by two main peaks: the one at shorter wavelengths corresponding to the PBG lower edge and the one inside the gap corresponding to the edge-state $\lambda_\ell(0.7\pi)=2469 \text{ nm}$. This is confirmed by the electric field spatial profile in Fig. 6c) for $t = 35 \text{ ps}$, which reveals the coexistence of an extended mode and a localization at $z \cong 4 \mu\text{m}$.

The US chain provides similar results. From eq.(4) and (1), for given N and Γ_o , the dipole coupling coefficient is fixed by $N\gamma^2 = w\Gamma_o\chi_A(\omega_o)$. On the other hand the Γ_o value allows to control the gap width $\Delta\omega = 2w_U\Gamma_o$ and the left-edge mode resonance $\omega_\ell = w_L\Gamma_o + \omega_o$. This circumstance allows a tunable field emission, either varying Γ_o or the pumping rate N . We choose $\xi = 0.5\pi$, furnishing $w = w_U = 0.4179$ and $w = w_L = -0.3465$ for the stop band upper edge and left-edge mode in Fig. 1b).

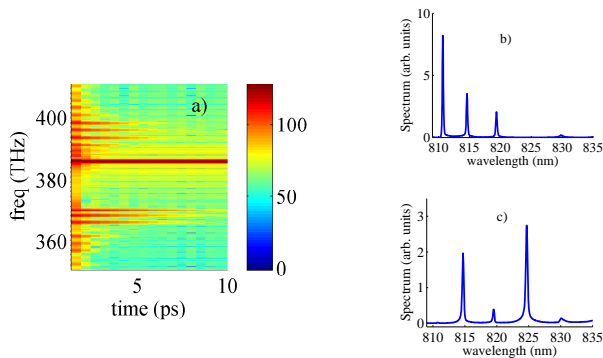


FIG. 7. a) Time-dependent spectrum of the output signal in the left side of the US chain. Emitted spectrum for b) $\Gamma_o = 5.89 \times 10^{-3} \text{ eV}$ and c) $\Gamma_o = 2.945 \times 10^{-2} \text{ eV}$

As shown in Fig. 7a) for $N=10^{23} \text{ m}^{-3}$ and $\Gamma_o = 5.89 \times 10^{-3} \text{ eV}$, stimulated emission starts to overtake the spontaneous one after a transient regime ($t \approx 3 \text{ ps}$) of laser field build-up. Once the steady state is reached the spectrogram of the emitted signal shows characteristic peaks. The peak at $\nu \approx 385 \text{ THz}$ corresponds to a delocalized mode. In addition, the optical feedback edge-mode localization gives rise to emission at $\nu_\ell=370.2 \text{ THz}$. For this system a wavelengths tuning of the emitted spectrum can be obtained changing the Γ_o value as shown in

Fig. 7b) for $\Gamma_o = 5.89 \times 10^{-3} \text{ eV}$ where $\lambda_\ell=810.2 \text{ nm}$ and 7c) $\Gamma_o = 2.945 \times 10^{-2} \text{ eV}$ where $\lambda_\ell=814 \text{ nm}$.

Conclusions — In this paper we have analyzed the time-resolved optical response to an ultrashort light pulse and focused on edge states detection in 1D resonant topological insulators given by two-level layers in uniform and modulated refractive index structures. For favorable system parameters obtained through linearized Maxwell-Bloch equations, we show that a direct observation of topological protected edge states can be achieved following the time evolution of the population inversion with different properties of uniform structures with respect to periodic systems. We provide evidence that a RTI can act as a resonator with laser like emissions due to localized edge modes; we also show that the emission frequency can be tuned by acting on the pumping energy or other system parameters.

An experimental test of our results is possible by the use of active TLS of quantum wells embedded in a semiconductor structure with periodically alternating linear index of refraction. In fact, for low densities, excitons in quantum wells can be considered as effective two-level systems if their resonance is close to the operating frequency. For these systems, the mechanism of emission is expected to have a low or vanishing laser threshold since, being the resonator directly etched in the amplifying material, an effective feedback can be obtained.

Using topologically protected states for lasing in resonant systems may open a variety of several new directions in laser physics. Achieving lasing-like action may be favored in regimes in which no feasible way for inversion population can be imagined as for example silicon lasers; in addition topologically protected states may also allow to have very narrow band emission because of the low coupling with radiation modes, proving extremely coherent sources at room temperature for metrological and spectroscopic applications.

We acknowledge support from the ERC project VANGUARD (grant number 664782), and the Templeton Foundation (grant number 58277).

-
- * Corresponding author: laura.pilozzi@isc.cnr.it
- [1] Aubry, S., André, G., *Ann. Israel. Phys. Soc.* **3**, 133 (1980)
- [2] P. G. Harper, *Proc. Phys. Soc., London, Sect. A* **68**, 874 (1955).
- [3] Anderson, P. W. , *Phys. Rev.* **109**, 1492, (1958).
- [4] K. Ishii, *Prog. Theor. Phys. Suppl.* **53**, 77 (1973)
- [5] D. J. Thouless, *Phys. Rep.* **13**, 95 (1974)
- [6] M. Verbin, O. Zilberberg, Y. E. Kraus, Y. Lahini and Y. Silberberg *Phys. Rev. Lett.* **110**,076403 (2013)
- [7] Zhaoju Yang, Fei Gao, Xihang Shi, Xiao Lin, Zhen Gao, Yidong Chong, Baile Zhang, *Phys. Rev. Lett.* **114**,114301 (2015)
- [8] Z.Wang, Y. Chong, J. D. Joannopoulos, and M. Soljacic *Nature* **461**, 772 (2009)
- [9] M. C. Rechtsman, J. M. Zeuner, Y. Plotnik, Y. Lumer, D. Podolsky, F. Dreisow, S. Nolte, M. Segev, and A. Szamei, *Nature* **496**, 196 (2013)
- [10] L. Lu, J. D. Joannopoulos, and M. Soljacic *Nature Photonics* **8**, 821 (2014)
- [11] Y. E. Kraus, Y. Lahini, Z. Ringel, M. Verbin, and O. Zilberberg, *Phys. Rev. Lett.* **109**, 106402 (2012)
- [12] S. Ganeshan, K. Sun, and S. Das Sarma, *Phys. Rev. Lett.* **110**, 180403 (2013)
- [13] G. Roati, C. D’Errico, L. Fallani, M. Fattori, C. Fort, M. Zaccanti, G. Modugno, M. Modugno, and M. Inguscio, *Nature (London)* **453**, 895 (2008)
- [14] A. N. Poddubny, L. Pilozzi, M. M. Voronov, and E. L. Ivchenko, *Phys. Rev. B* **77**, 113306 (2008)
- [15] A. N. Poddubny, L. Pilozzi, M. M. Voronov, and E. L. Ivchenko, *Phys. Rev. B* **80** 115314 (2009)
- [16] A. V. Poshakinskiy, al., *Phys. Rev. Lett.* **112**, 107403 (2014).
- [17] T. Karzig, al., *Phys. Rev. X* **5**, 031001 (2015).
- [18] A. Taflove and S. C. Hagness, *Computational Electrodynamics: The Finite-Difference Time-Domain Method* (Artech House, Boston, 2005).
- [19] Richard W. Ziolkowski, John M. Arnold, Daniel M. Gogny, *Phys. Rev. A.* **52**, 3082 (1995).
- [20] V. Folli, C. Conti, *J. Opt. Soc. Am. B* **29**, 2080 (2012).
- [21] A. V. Poshakinskiy, A. N. Poddubny, M. Hafezi *Phys. Rev. A* **91**, 043830, (2015).
- [22] C. Conti, A. Fratalocchi, *Nat. Phys.* **4**, 794 (2008).
- [23] G. Slavcheva, J. Arnold, and R. Ziolkowski, *IEEE J. Sel. Top. Quantum Electron.* **10**, 1052 (2004)
- [24] S. L. McCall and E. L. Hahn, *Phys. Rev. Lett.* **18**, 908 (1967).
- [25] Li-Jun Lang, Xiaoming Cai, and Shu Chen *Phys. Rev. Lett.* **108**, 220401 (2012).
- [26] L. Dal Negro, C. J. Oton et al. *Phys. Rev. Lett.* **90**, 055501 (2003).